Research Article | Vol. 28, No. 14 / 6 July 2020 / Optics Express 21182

Optics EXPRESS

Measuring the rotational temperature and pump intensity in molecular alignment experiments via high harmonic generation

YANQING HE,[1] LIXIN HE,[1,3] PU WANG,[1] BINCHENG WANG,[1] SIQI SUN,[1] RUXUAN LIU,[1] BAONING WANG,[1] PENGFEI LAN,[1,4] AND PEIXIANG LU[1,2,5]

[1]*Wuhan National Laboratory for Optoelectronics and School of Physics, Huazhong University of Science and Technology, Wuhan 430074, China*
[2]*Hubei Key Laboratory of Optical Information and Pattern Recognition, Wuhan Institute of Technology, Wuhan 430205, China*
[3]*helx_hust@mail.hust.edu.cn*
[4]*pengfeilan@mail.hust.edu.cn*
[5]*lupeixiang@mail.hust.edu.cn*

Abstract: We demonstrate a method to simultaneously measure the rotational temperature and pump intensity in laser-induced molecular alignment by the time-resolved high harmonic spectroscopy (HHS). It relies on the sensitive dependence of the arising times of the local minima and maxima of the harmonic yields at the rotational revivals on the pump intensity and rotational temperature. By measuring the arising times of these local extrema from the time-resolved harmonic signals, the rotational temperature and pump intensity can be accurately measured. We have demonstrated our method using N_2 molecules. The validity and robustness of our method are tested with different harmonic orders and by changing the gas pressures as well as the distance between the gas exit and the optical axis. Moreover, we have also demonstrated the versatility of our method by applying it to CO_2 molecules.

1. Introduction

Molecular alignment and orientation [1–6] by ultrashort pulse laser play an important role in molecular collision and reaction dynamics, and have been of great interests of both physicists and chemists for their widespread applications in many areas, varying from multiphoton ioization [7,8], ultrashort pulse compression [9,10], molecular orbital reconstruction [11–13], control and imaging of chemical reactions [14–16], charge migration [17] and high harmonic generation (HHG) [18–25]. Generally, an intense nonresonant laser pulse has proved to be the most versatile method to obtain molecular alignment. Impulsively excited by a pump laser, the induced molecular rotational dynamics can be well understood in two steps: First, the pump laser interacts with the molecules and create molecular rotational wave packet (RWP) through stimulated Raman transitions [1], leading to temporary alignment of the molecules in a narrow cone around the polarization direction; Second, the created RWP disperses and evolves under the field-free condition. Owing to the time-dependent phase beating of the coherently populated rotational states, recurrence of alignment and antialignment appears at the rotational revivals.

In molecular alignment, the induced rotational dynamics are mainly determined by two factors. One is the rotational temperature, which determines the initial thermal distribution of the rotational states. The other one is the pump laser, which determines the redistribution of the rotational states after the laser-molecule interaction. Previously, several methods have reported to measure the rotational temperature. For example, the coherent anti-Stokes Raman scattering (CARS) [26–28] and degenerate four-wave mixing [29] are two powerful methods. Nevertheless,

#397560 https://doi.org/10.1364/OE.397560
Journal © 2020 Received 13 May 2020; revised 20 Jun 2020; accepted 26 Jun 2020; published 1 Jul 2020

Optics EXPRESS

they have limitations when, for instance, the signal frequencies are close to those of the laser pulses. In recent years, several studies demonstrated that the degree of molecular alignment depends sensitively on the pump intensity and the rotational temperature [30,31]. Moreover, Loriot *et al.* found that the time interval between the delocalization and alignment is correlated to the pump intensity and rotational temperature [32], which therefore provides a promising way for estimating the intensity and temperature in molecular alignment experiment. Recently, Yoshii *et al.* demonstrated the measurement of rotational temperature in the experiment of HHG from aligned molecules [33]. In their work, the rotational temperature is derived from the Fourier spectrum of measured time-resolved HHG signals by a fitting process in theory. In this regard, the parameters of the pump laser, especially the pump intensity, are assumed to be already known. Although the pulse duration can be obtained by an optical autocorrelator or a frequency-resolved optical gating (FROG) equipment [34] and the laser frequency can be measured by a spectrometer, an accurate measurement of the laser intensity has been a longstanding and arduous task [35–37].

In this paper, we propose an improved method to simultaneously measure the rotational temperature and pump intensity in molecular HHG experiment. In our experiment, we adopt a pump-probe system, where the pump pulse is applied to align the molecules and the intense probe pulse is used to interact with the molecules to generate high harmonic radiations [38,39]. The HHG signal is measured as a function of the time delay between the pump and probe pulses. From the measured HHG signals, we find that the arising times of the local maxima and minima of the HHG yields at the rotational revivals show strong dependence on the rotational temperature and pump intensity. Following this feature, one can take an *in-situ* measurement of both the rotational temperature and pump intensity synchronously. With this method, we have successfully measured the rotational temperature and pump intensity in a N_2 flow. The measured results are consistent for different harmonic orders and show good agreement with the nature of adiabatic expansion of a gas flow when the gas pressure and the distance between the gas exit and the optical axis are changed. These results prove our method to be valid and robust. Moreover, due to the universality of nonadiabatic molecular alignment by nonresonant femtosecond laser, our method can also be applied to other molecules except spherical-top molecules.

2. Results and discussion

2.1. Experimental details

Figure 1(a) displays the schematic of our experimental setup. The experiment is carried out by using a commercial Ti:sapphire laser system (Astrella-USP-1K, Coherent, Inc.). It delivers laser pulses at a repetition rate of 1 kHz. The pulse duration and the central wavelength of the laser are measured to be 35-fs and 800 nm, respectively. The output laser is split by a beam splitter to produce the pump and probe pulses. The pump pulse is used firstly to create the molecular RWP. Subsequently, the intense probe pulse with adjustable time delay interacts with the molecular ensemble to generate high harmonic radiations. These two pulses are focused into a gas nozzle by a convex lens with a 300-mm focal length. The nozzle with a diameter of 250 μm is mounted on a motorized stage, which is used to adjust the distance (defined as x) between the gas exit and the optical axis. The generated HHG signal is detected by a homemade flat-field soft x-ray spectrometer [24].

To demonstrate our scheme, we choose N_2 molecule as a prototype. The measured time-dependent HHG signals (blue dots) of harmonic 21 (H21) is shown in Fig. 1(b). Here, the gas pressure is 8.58×10^4 Pa and the two pulses are focused at the position of $x = 0.2$ mm. From Fig. 1(b), one can see obvious local maxima and minima at the full and fractional rotational revivals, e.g., around 8.4 ps (1 T_{rev}, where $T_{rev} = \frac{1}{2B_0c}$ is the revival period with B_0 the rotational constant and c the velocity of light.) and 4.2 ps ($\frac{1}{2}$ T_{rev}). For N_2, the HHG signal is the most prominent when the molecular axis is parallel to the laser polarization due to the σ_g symmetry of

Optics EXPRESS

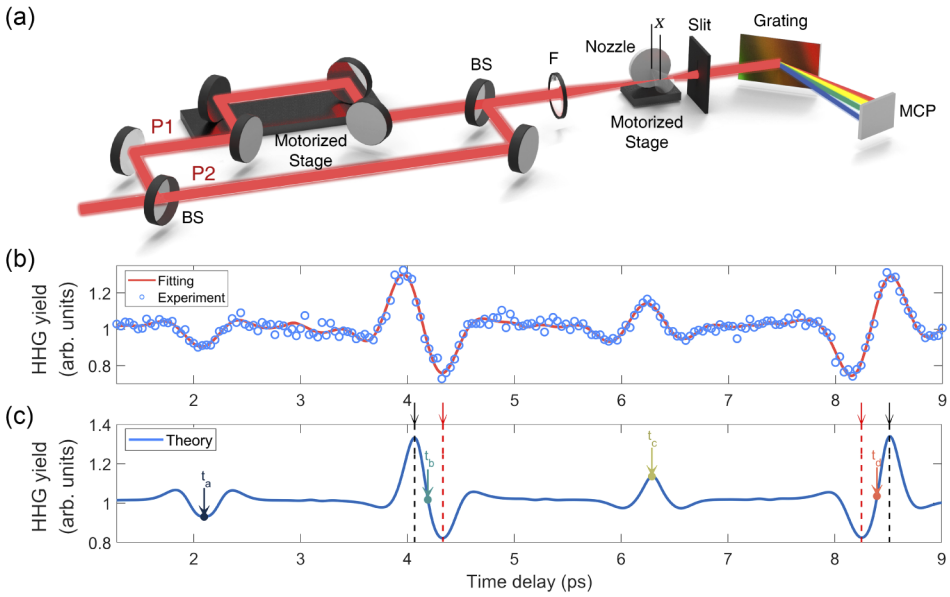

Fig. 1. (a) Schematic diagram of the experimental setup. (b) Measured HHG signal of H21 (blue dots) from N_2 molecule as a function of the pump-probe time delay. The solid line is the fitting result. (c) Same as (b), but for theoretical result simulated with the rotational temperature of 100 K and the pump intensity of 3.5×10^{13} W/cm^2 . t_a, t_b, t_c, t_d pointed out by arrows are four characteristic times, which are independent of the rotational temperature and the pump intensity. The dashed lines together with arrows on top indicate the arising times of local extrema of HHG yields at rotational revivals.

its highest occupied molecular orbital (HOMO) [40,41]. The local maximum implies that most molecules are aligned parallel to the pump pulse polarization, indicating an alignment revival. While the local minimum corresponds to an alignment perpendicular to the laser polarization, i.e., an antialignment revival.

2.2. *Extracting rotational temperature and pump intensity from time-resolved HHG signals*

To extract the pump intensity and rotational temperature from the measurements, we have calculated the time-dependent HHG yields with series of rotational temperatures (T_{rot}) and pump intensities (I_{pump}). In our calculations, we first numerically solve the time-dependent Schrödinger equation of the molecular RWP [2], which is

$$i\frac{\partial \Psi_{JM}(\theta,\phi,t)}{\partial t} = [B_e\mathbf{J}^2 - \frac{1}{4}(\alpha_{\parallel}cos^2\theta + \alpha_{\perp}sin^2\theta)E(t)^2]\Psi_{JM}(\theta,\phi,t). \quad (1)$$

where $\mathbf{J}$ is the rotation operator, and B_e is the rotational constant of the molecules. θ and ϕ are the polar and azimuthal angles of molecular axis. $\alpha_{\parallel}$ and $\alpha_{\perp}$ are the components of polarizability tensor which are parallel and perpendicular to the molecular axis, respectively. $E(t)$ is the envelop of the electric field of the pump laser. Equation (1) can be solved with the split-operator method [42] for each initial rotational state $|JM\rangle$. Assuming a thermal distribution of the initial rotational states, the time-dependent molecular axis distribution $\rho(\theta,\phi,t)$ can be written as a weighted average of the squared modulus of the wave packet $\Psi_{JM}(\theta,\phi,t)$ [2,43–47], i.e.,

$$\rho(\theta,\phi,t) = \sum_{JM}\Gamma_{JM}|\Psi_{JM}(\theta,\phi,t)|^2, \quad (2)$$

Optics EXPRESS

where Γ_{JM} is the population of the initial state $|JM\rangle$ given by the Boltzmann distribution. HHG from the impulsively excited molecular ensemble can be related to the single-molecule contribution through the time-dependent molecular angular distribution $\rho(\theta, \phi, t)$. Considering the coherent nature of HHG, the time-dependent HHG yield will thus be given by [45,47]:

$$I_q(t) = \left| \int_{\phi=0}^{2\pi} \int_{\theta=0}^{\pi} S_q(\theta) \rho(\theta, \phi, t) \sin\theta d\theta d\phi \right|^2 . \quad (3)$$

Here, $S_q(\theta)$ is the induced dipole moment of the q-th harmonic related to the single molecule response with given orientation. In our calculation, the single molecule dipole moment $S_q(\theta)$ is obtained by using the quantitative rescattering (QRS) theory [47,48], of which the accuracy and validity in modeling molecular HHG have been well established. Considering the laser intensity is strongest at the center of the focal spot, the corresponding harmonic radiation is most prominent. In our simulation, the focal volume effect is ignored and only the harmonic radiation at the center of the focal spot is considered. Figure 1(c) presents an example of the numerical HHG result, which is calculated at T_{rot} = 100 K and $I_{pump} = 3.5 \times 10^{13}$ W/cm^2.

From the calculation results, we notice that the arising times of the local maxima (t_{max}) and minima (t_{min}) of the HHG yields [i.e., the local extrema pointed out by dashed lines and arrows on top at rotational revivals in Fig. 1(c)] show significant dependence on both the rotational temperature and pump intensity. For instance, in Figs. 2(a) and 2(b), we plot the arising times of the local maximum ($t_{max}^{1/2}$) and local minimum ($t_{min}^{1/2}$) around $\frac{1}{2}$ T_{rev} as a function of the rotational temperature and pump intensity. It is shown that, as the rotational temperature or pump intensity increases, $t_{max}^{1/2}$ is delayed [see Fig. 2(a)]. While $t_{min}^{1/2}$ shows an opposite dependence, it is advanced as the rotational temperature or pump intensity increases [see Fig. 2(b)]. On the other hand, we find four characteristic times, i.e., t_a, t_b, t_c and t_d indicated by arrows in Fig. 1(c), in one revival, where t_a (t_c) refers to the local minimum (maximum) at $\frac{1}{4}$ T_{rev} ($\frac{3}{4}$ T_{rev}), t_b (t_d) the midpoint between t_{max} and t_{min} at $\frac{1}{2}$ T_{rev} (1 T_{rev}). These four characteristic times are found to be independent of the pump intensity and rotational temperature. As a result, they can be used to calibrate the time delays measured in the experiment. In our work, we use t_a and t_d to do the calibration, because they are easy to be identified (local minimum and maximum) in experiment. In Fig. 1(b), the time delay (the horizontal axis) has been already calibrated. To extract the arising times of the local maxima and minima precisely, we fit the time-dependent HHG signal by the least squares method. The fitting result is shown as the red line in Fig. 1(b). From the fitting curve, the arising times of local maximum and minimum around $\frac{1}{2}$ T_{rev} are acquired to be 4.024 ps and 4.388 ps, respectively. Further, we pick out all combinations of the rotational temperatures and pump intensities that lead to $t_{max}^{1/2}$ = 4.024 ps. The result is shown as the solid line in Fig. 2(a). Similarly, we have also picked out the combinations of rotational temperatures and pump intensities for $t_{min}^{1/2}$ = 4.388 ps. The corresponding result is shown as the dotted line in Fig. 2(b). By putting these two contour lines together [see Fig. 2(c)], the resultant intersection point just corresponds to the pending rotational temperature and pump intensity. In our experiment, these two parameters extracted from the signal of H21 in Fig. 1(b) are 32.01 ± 1.45 K and (4.45 ± 0.13) × 10^{13} W/cm^2, respectively.

2.3. Validity and universality of the method

To check the reliability of the extracted result, we apply our method repeatedly to other harmonic orders ranging from H15 to H19. The results are displayed in Fig. 3. It can be seen that the measured rotational temperatures and pump intensities are nearly the same for different harmonic orders. This result is consistent with the nature that HHG is a much faster process than molecular rotation. The rotational state of the molecules can be considered unchanged during the HHG process.

Optics EXPRESS

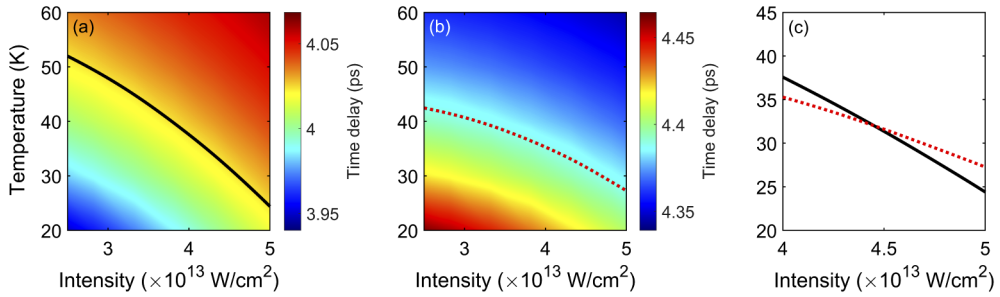

Fig. 2. (a) The arising time of the local maximum $t_{max}^{1/2}$ at $\frac{1}{2}\ T_{rev}$ for N_2 molecule as a function of the rotational temperature and pump intensity. The black line is a contour line for $t_{max}^{1/2} = 4.024$ ps. (b) Same as (a), but for the arising time of local minimum $t_{min}^{1/2}$ at $\frac{1}{2}\ T_{rev}$. The red dotted line is a contour line for $t_{min}^{1/2} = 4.388$ ps. (c) Contour lines for $t = 4.024$ ps (solid line) and $t = 4.388$ ps (dotted line). The intersection indicates the pending rotational temperature and pump intensity.

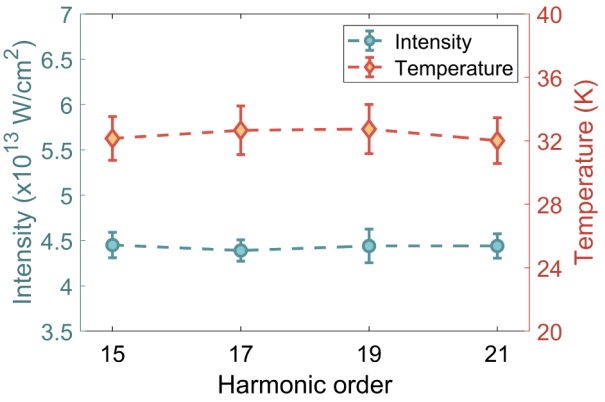

Fig. 3. The measured rotational temperature and pump intensity as a function of harmonic order. Here, the error bars of both results represent the standard deviation of five independent measurements.

Besides, we have performed more experiments to confirm the validity of our method. In Fig. 4, the rotational temperature and pump intensity have been measured for different gas pressures using the time-dependent signal of H21. One can see that the pump intensity remains constant with the gas pressure increasing, which is consistent with the experimental condition. While the measured temperature decreases with the increase of the gas pressure. In addition, we have also performed the experiment by changing the distance x. The measured rotational temperature and pump intensity as a function of x are displayed in Fig. 5. It shows that the pump intensity is still unchanged, while the rotational temperature drops with the increase of x. The results are consistent with previous works [33,49–52].

Finally, our method is versatile and can be applied to other molecules. To demonstrate this point, we have performed experiments with CO_2 molecules. Figure 6(a) shows the measured results of H25. Here, the laser intensity and gas pressure are maintained the same as in Fig. 1(b). From Fig. 6(a), one can also see a strong delay dependence of the HHG signals at the rotational revivals (e.g. around $t = 21.2$ and 42.4 ps). Due to the more complex scattering cross section and the different symmetry of HOMO (π_μ), the modulations of the time-dependent HHG signals of CO_2 are opposite to that of N_2. Similar to N_2, we choose the arising times of the local

Optics EXPRESS

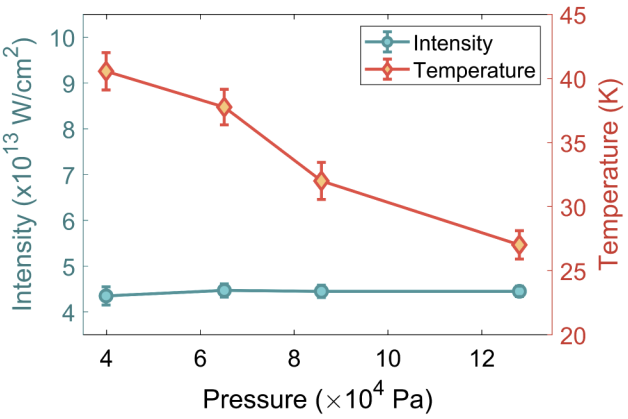

Fig. 4. The measured rotational temperature and pump intensity as a function of pressure. Here, the error bars of both results represent the standard deviation of five independent measurements.

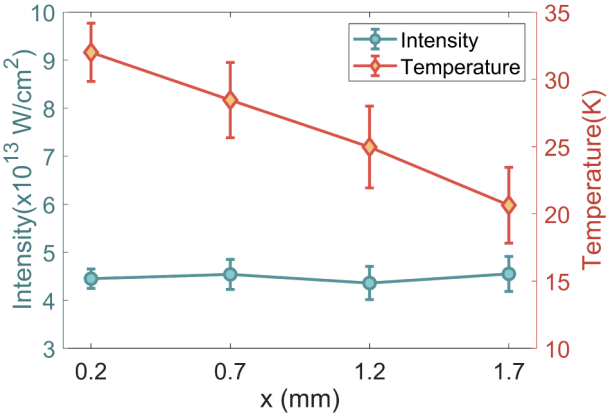

Fig. 5. The measured rotational temperature and pump intensity as a function of distance x. Here, the error bars of both results represent the standard deviation of five independent measurements.

minimum and maximum [pointed out by black and red arrows together with dashed lines in Fig. 6(a), respectively] around $\frac{1}{2}\ T_{rev}$ to do the extraction. For CO_2, $t_{min}^{1/2}$ and $t_{max}^{1/2}$ obtained from the fitting curve [yellow line in Fig. 6(a)] of the measured HHG signals are 21.013 ps and 21.791 ps, respectively. In Figs. 6(b) and 6(c), we show the calculated $t_{min}^{1/2}$ and $t_{max}^{1/2}$ as a function of the rotational temperature and pump intensity. One can see that $t_{min}^{1/2}$ and $t_{max}^{1/2}$ have opposite dependence as the rotational temperature or the pump intensity varies. We further pick out the combinations of rotational temperatures and pump intensities that lead to $t_{min}^{1/2} = 21.013$ ps and $t_{max}^{1/2} = 21.791$ ps. Corresponding results are shown as the solid and dotted lines in Figs. 6(b) and 6(c), respectively. Based on these two contour lines, the resultant rotational temperature and pump intensity are 40.28 ± 1.39 K and $(4.58 \pm 0.14) \times 10^{13}$ W/cm^2, respectively [see Fig. 6(d)]. It's worth mentioning that, the pump intensity and rotational temperature can be determined by any two local extrema at the rotational revivals if they obey opposite dependence on T_{rot} and I_{pump}. As an example, we select an alternative local extremum, i.e., the local minimum around $\frac{1}{4}\ T_{rev}$ [$t_{min}^{1/4}$, indicated by green arrow together with dashed line in Fig. 6(a)], instead of $t_{max}^{1/2}$ to

Optics EXPRESS

do the extraction. In our experiment, $t_{min}^{1/4}$ is measured to be 11.502 ps. Figure 7(a) displays the calculated $t_{min}^{1/4}$ as a function of T_{rot} and I_{pump}. The dependence of $t_{min}^{1/4}$ on T_{rot} and I_{pump} is similar to that of $t_{max}^{1/2}$ in Fig. 6(c), but is opposite to that of $t_{min}^{1/2}$ in Fig. 6(b). With the contour lines of $t_{min}^{1/4}$ and $t_{min}^{1/2}$, the rotational temperature and pump intensity can also be determined [see Fig. 7(b)], which are 41.54 ± 1.46 K and $(4.48 \pm 0.18) \times 10^{13}$ W/cm^2, respectively. This result is quite close to that obtained by $t_{min}^{1/2}$ and $t_{max}^{1/2}$.

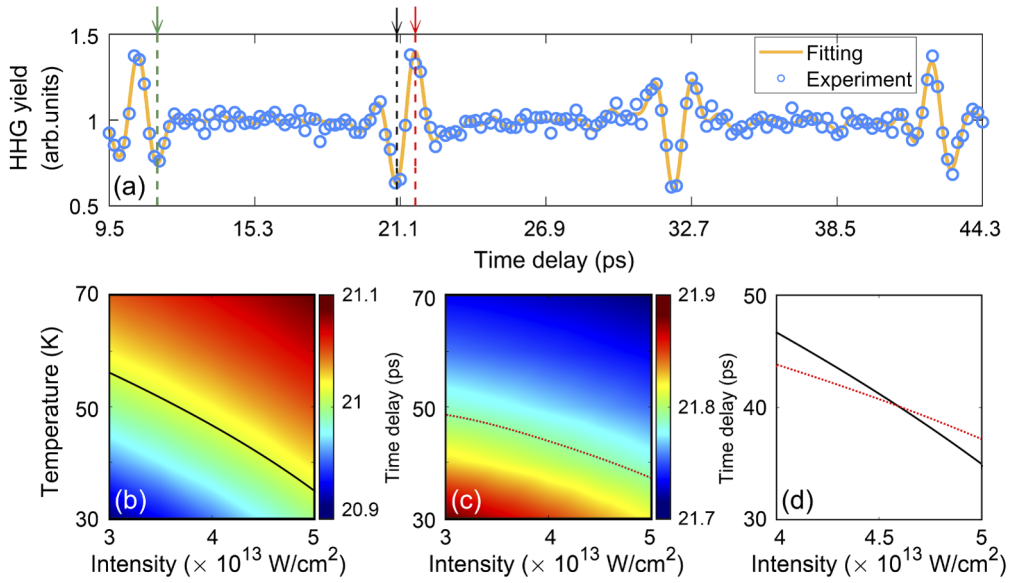

Fig. 6. (a) Measured HHG signal of H25 (blue dots) from CO_2 molecule as a function of the pump-probe time delay. The solid line is the fitting result. The dashed lines together with arrows on top indicate the arising times of local extrema of HHG yields at rotational revivals. (b) The arising time of local minimum $t_{min}^{1/2}$ at $\frac{1}{2}$ T_{rev} as a function of the rotational temperature and pump intensity. The black line is a contour line for $t_{min}^{1/2}$ = 21.013 ps. (c) Same as (b), but for the arising time of local maximum $t_{max}^{1/2}$ at $\frac{1}{2}$ T_{rev}. The red dotted line is a contour line for $t_{max}^{1/2}$ = 21.791 ps. (d) Contour lines for t = 21.013 ps (solid line) and t = 21.791 ps (dotted line). The intersection indicates the pending rotational temperature and pump intensity.

Optics EXPRESS

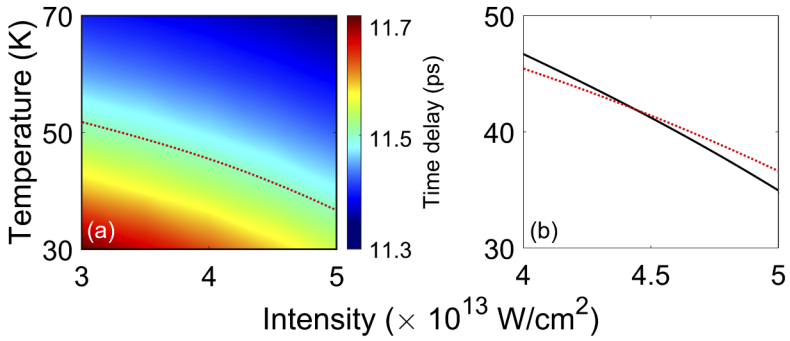

Fig. 7. (a) The arising time of the local minimum $t_{min}^{1/4}$ at $\frac{1}{4}$ T_{rev} for CO_2 molecule as a function of the rotational temperature and pump intensity. The red dotted line is a contour line for $t_{min}^{1/4}$ = 11.502 ps. (b) Contour lines for t = 21.013 ps (solid line) and t = 11.502 ps (dotted line). The intersection indicates the pending rotational temperature and pump intensity.

3. Conclusion

In summary, we demonstrate a technique to achieve an *in-situ* measurement of the rotational temperature and pump intensity synchronously in molecular HHG experiment. From the time-dependent HHG signals of N_2 molecule, we find that the arising times of the local minima and maxima of the harmonic yield have sensitive dependence on the rotational temperature and pump intensity. This feature enables us to directly determine the rotational temperature and pump intensity from the time-dependent HHG signals simultaneously. The accuracy of our method is confirmed by using different harmonic orders. Moreover, the measured results with different gas pressure and distances between the gas exit and the optical axis agree well with the nature of adiabatic expanding of a gas flow, which proves the validity of our method. Since the laser-induced alignment can generally be applied to different kinds of molecules, our method can be applied to other molecules (except spherical-top molecules) as well. Such versatility is confirmed by the experiment with CO_2 molecule. Besides, we have also proved that the rotational temperature and pump intensity can be determined by any two local extrema which follow contrary dependence on the rotational temperature and pump intensity. Such flexibility makes our method more convenient in practical application.

Funding

National Key Research and Development Program of China (2017YFE0116600, 2019YFA0308300); National Natural Science Foundation of China (11627809, 11704137, 11774109, 11874165); Fundamental Research Funds for the Central Universities (2017KFXKJC002); Program for HUST Academic Frontier Youth Team; Science and Technology Planning Project of Guangdong Province (2018B090944001).

Disclosures

The authors declare no conflicts of interest.

References

1. L. Cai, J. Marango, and B. Friedrich, "Time-dependent alignment and orientation of molecules in combined electrostatic and pulsed nonresonant laser fields," Phys. Rev. Lett. **86**(5), 775–778 (2001).
2. H. Stapelfeldt and T. Seideman, "Colloquium: Aligning molecules with strong laser pulses," Rev. Mod. Phys. **75**(2), 543–557 (2003).

Optics EXPRESS

3. O. Ghafur, A. Rouzée, A. Gijsbertsen, W. K. Siu, S. Stolte, and M. J. J. Vrakking, "Impulsive orientation and alignment of quantum-state-selected NO molecules," Nat. Phys. **5**(4), 289–293 (2009).
4. Y. Ohshima and H. Hasegawa, "Coherent rotational excitation by intense nonresonant laser fields," Int. Rev. Phys. Chem. **29**(4), 619–663 (2010).
5. K. Lin, I. Tutunnikov, J. Qiang, J. Ma, Q. Song, Q. Ji, W. Zhang, H. Li, F. Sun, X. Gong, H. Li, P. Lu, H. Zeng, Y. Prior, I. S. Averbukh, and J. Wu, "All-optical field-free three-dimensional orientation of asymmetric-top molecules," Nat. Commun. **9**(1), 5134 (2018).
6. E. Karamatskos, S. Raabe, T. Mullins, A. Trabattoni, P. Stammer, G. Goldsztejn, R. Johansen, K. Długołecki, H. Stapelfeldt, M. J. J. Vrakking, S. Trippel, A. Rouzée, and J. Küpper, "Molecular movie of ultrafast coherent rotational dynamics of OCS," Nat. Commun. **10**(1), 3364 (2019).
7. I. V. Litvinyuk, K. F. Lee, P. W. Dooley, D. M. Rayner, D. M. Villeneuve, and P. B. Corkum, "Alignment-dependent strong field ionization of molecules," Phys. Rev. Lett. **90**(23), 233003 (2003).
8. T. K. Kjeldsen, C. Z. Bisgaard, L. B. Madsen, and H. Stapelfeldt, "Role of symmetry in strong-field ionization of molecules," Phys. Rev. A **68**(6), 063407 (2003).
9. J. Wu, H. Cai, H. Zeng, and A. Couairon, "Femtosecond filamentation and pulse compression in the wake of molecular alignment," Opt. Lett. **33**(22), 2593–2595 (2008).
10. R. A. Bartels, T. C. Weinacht, N. Wagner, M. Baertschy, C. H. Greene, M. M. Murnane, and H. C. Kapteyn, "Phase modulation of ultrashort light pulses using molecular rotational wave packets," Phys. Rev. Lett. **88**(1), 013903 (2001).
11. J. Itatani, J. Levesque, D. Zeidler, H. Niikura, H. Pépin, J. C. Kieffer, P. B. Corkum, and D. M. Villeneuve, "Tomographic imaging of molecular orbitals," Nature **432**(7019), 867–871 (2004).
12. C. Vozzi, M. Negro, F. Calegari, G. Sansone, M. Nisoli, S. De Silvestri, and S. Stagira, "Generalized molecular orbital tomography," Nat. Phys. **7**(10), 822–826 (2011).
13. C. Zhai, X. Zhang, X. Zhu, L. He, Y. Zhang, B. Wang, Q. Zhang, P. Lan, and P. Lu, "Single-shot molecular orbital tomography with orthogonal two-color fields," Opt. Express **26**(3), 2775–2784 (2018).
14. J. J. Larsen, I. Wendt-Larsen, and H. Stapelfeldt, "Controlling the branching ratio of photodissociation using aligned molecules," Phys. Rev. Lett. **83**(6), 1123–1126 (1999).
15. C. Z. Bisgaard, O. J. Clarkin, G. Wu, A. M. Lee, O. Geßner, C. C. Hayden, and A. Stolow, "Time-resolved molecular frame dynamics of fixed-in-space CS_2 molecules," Science **323**(5920), 1464–1468 (2009).
16. C. B. Madsen, L. B. Madsen, S. S. Viftrup, M. P. Johansson, T. B. Poulsen, L. Holmegaard, V. Kumarappan, K. A. Jørgensen, and H. Stapelfeldt, "Manipulating the torsion of molecules by strong laser pulses," Phys. Rev. Lett. **102**(7), 073007 (2009).
17. P. M. Kraus, B. Mignolet, D. Baykusheva, A. Rupenyan, L. Horný, E. F. Penka, G. Grassi, O. I. Tolstikhin, J. Schneider, F. Jensen, L. B. Madsen, A. D. Bandrauk, F. Remacle, and H. J. Wörner, "Measurement and laser control of attosecond charge migration in ionized iodoacetylene," Science **350**(6262), 790–795 (2015).
18. R. Velotta, N. Hay, M. B. Mason, M. Castillejo, and J. P. Marangos, "High-order harmonic generation in aligned molecules," Phys. Rev. Lett. **87**(18), 183901 (2001).
19. N. Hay, R. Velotta, M. Lein, R. de Nalda, E. Heesel, M. Castillejo, and J. P. Marangos, "High-order harmonic generation in laser-aligned molecules," Phys. Rev. A **65**(5), 053805 (2002).
20. J. Itatani, D. Zeidler, J. Levesque, M. Spanner, D. M. Villeneuve, and P. B. Corkum, "Controlling high harmonic generation with molecular wave packets," Phys. Rev. Lett. **94**(12), 123902 (2005).
21. T. Kanai, S. Minemoto, and H. Sakai, "Ellipticity dependence of high-order harmonic generation from aligned molecules," Phys. Rev. Lett. **98**(5), 053002 (2007).
22. S. Ramakrishna and T. Seideman, "Information content of high harmonics generated from aligned molecules," Phys. Rev. Lett. **99**(11), 113901 (2007).
23. A. Rupenyan, J. B. Bertrand, D. M. Villeneuve, and H. J. Wörner, "All-optical measurement of high-harmonic amplitudes and phases in aligned molecules," Phys. Rev. Lett. **108**(3), 033903 (2012).
24. Y. He, L. He, P. Lan, B. Wang, L. Li, X. Zhu, W. Cao, and P. Lu, "Direct imaging of molecular rotation with high-order-harmonic generation," Phys. Rev. A **99**(5), 053419 (2019).
25. B. Wang, L. He, Y. He, Y. Zhang, R. Shao, P. Lan, and P. Lu, "All-optical measurement of high-order fractional molecular echoes by high-order harmonic generation," Opt. Express **27**(21), 30172–30181 (2019).
26. P. Huber-Wälchli, D. M. Guthals, and J. W. Nibler, "Cars spectra of supersonic molecular beams," Chem. Phys. Lett. **67**(2-3), 233–236 (1979).
27. M. D. Duncan, P. Österlin, and R. L. Byer, "Pulsed supersonic molecular-beam coherent anti-stokes raman spectroscopy of C_2H_2," Opt. Lett. **6**(2), 90–92 (1981).
28. T. Lang, M. Motzkus, H. M. Frey, and P. Beaud, "High resolution femtosecond coherent anti-stokes raman scattering: Determination of rotational constants, molecular anharmonicity, collisional line shifts, and temperature," J. Chem. Phys. **115**(12), 5418–5426 (2001).
29. T. Hornung, H. Skenderović, K.-L. Kompa, and M. Motzkus, "Prospect of temperature determination using degenerate four-wave mixing with sub-20 fs pulses," J. Raman Spectrosc. **35**(11), 934–938 (2004).
30. E. Péronne, M. D. Poulsen, C. Z. Bisgaard, H. Stapelfeldt, and T. Seideman, "Nonadiabatic alignment of asymmetric top molecules: Field-free alignment of iodobenzene," Phys. Rev. Lett. **91**(4), 043003 (2003).
31. E. Péronne, M. D. Poulsen, H. Stapelfeldt, C. Z. Bisgaard, E. Hamilton, and T. Seideman, "Nonadiabatic laser-induced alignment of iodobenzene molecules," Phys. Rev. A **70**(6), 063410 (2004).

Optics EXPRESS

32. V. Loriot, P. Tzallas, E. P. Benis, E. Hertz, B. Lavorel, D. Charalambidis, and O. Faucher, "Laser-induced field-free alignment of the OCS molecule," J. Phys. B: At., Mol. Opt. Phys. **40**(12), 2503–2510 (2007).
33. K. Yoshii, G. Miyaji, and K. Miyazaki, "Measurement of molecular rotational temperature in a supersonic gas jet with high-order harmonic generation," Opt. Lett. **34**(11), 1651–1653 (2009).
34. R. Trebino, K. W. DeLong, D. N. Fittinghoff, J. N. Sweetser, M. A. Krumbügel, B. A. Richman, and D. J. Kane, "Measuring ultrashort laser pulses in the time-frequency domain using frequency-resolved optical gating," Rev. Sci. Instrum. **68**(9), 3277–3295 (1997).
35. A. S. Alnaser, X. M. Tong, T. Osipov, S. Voss, C. M. Maharjan, B. Shan, Z. Chang, and C. L. Cocke, "Laser-peak-intensity calibration using recoil-ion momentum imaging," Phys. Rev. A **70**(2), 023413 (2004).
36. C. Smeenk, J. Z. Salvail, L. Arissian, P. B. Corkum, C. T. Hebeisen, and A. Staudte, "Precise *in-situ* measurement of laser pulse intensity using strong field ionization," Opt. Express **19**(10), 9336–9344 (2011).
37. S. Xu, X. Sun, B. Zeng, W. Chu, J. Zhao, W. Liu, Y. Cheng, Z. Xu, and S. L. Chin, "Simple method of measuring laser peak intensity inside femtosecond laser filament in air," Opt. Express **20**(1), 299–307 (2012).
38. M. Kaku, K. Masuda, and K. Miyazaki, "Observation of revival structure in femtosecond-laser-induced alignment of N_2 with high-order harmonic generation," Jpn. J. Appl. Phys. **43**(No. 4B), L591–L593 (2004).
39. K. Miyazaki, M. Kaku, G. Miyaji, A. Abdurrouf, and F. H. M. Faisal, "Field-free alignment of molecules observed with high-order harmonic generation," Phys. Rev. Lett. **95**(24), 243903 (2005).
40. B. K. McFarland, J. P. Farrell, P. H. Bucksbaum, and M. Gühr, "High harmonic generation from multiple orbitals in N_2," Science **322**(5905), 1232–1235 (2008).
41. A.-T. Le, R. R. Lucchese, and C. D. Lin, "Uncovering multiple orbitals influence in high harmonic generation from aligned N_2," J. Phys. B: At., Mol. Opt. Phys. **42**(21), 211001 (2009).
42. S. Saugout, E. Charron, and C. Cornaggia, "H_2 double ionization with few-cycle laser pulses," Phys. Rev. A **77**(2), 023404 (2008).
43. S. Fleischer, Y. Khodorkovsky, Y. Prior, and I. S. Averbukh, "Controlling the sense of molecular rotation," New J. Phys. **11**(10), 105039 (2009).
44. K. Lin, Q. Song, X. Gong, Q. Ji, H. Pan, J. Ding, H. Zeng, and J. Wu, "Visualizing molecular unidirectional rotation," Phys. Rev. A **92**(1), 013410 (2015).
45. K. Lin, P. Lu, J. Ma, X. Gong, Q. Song, Q. Ji, W. Zhang, H. Zeng, J. Wu, G. Karras, G. Siour, J.-M. Hartmann, O. Faucher, E. Gershnabel, Y. Prior, and I. S. Averbukh, "Echoes in space and time," Phys. Rev. X **6**(4), 041056 (2016).
46. L. He, P. Lan, A.-T. Le, B. Wang, B. Wang, X. Zhu, P. Lu, and C. D. Lin, "Real-time observation of molecular spinning with angular high-harmonic spectroscopy," Phys. Rev. Lett. **121**(16), 163201 (2018).
47. C. D. Lin, A.-T. Le, Z. Chen, T. Morishita, and R. Lucchese, "Strong-field rescattering physics—self-imaging of a molecule by its own electrons," J. Phys. B: At., Mol. Opt. Phys. **43**(12), 122001 (2010).
48. A.-T. Le, R. R. Lucchese, S. Tonzani, T. Morishita, and C. D. Lin, "Quantitative rescattering theory for high-order harmonic generation from molecules," Phys. Rev. A **80**(1), 013401 (2009).
49. F. Huisken and T. Pertsch, "Coherent anti-stokes raman spectroscopy (CARS) of the ν_3 band of methane in supersonic molecular beams," Appl. Phys. B **41**(3), 173–178 (1986).
50. H.-D. Barth, C. Jackschath, T. Pertsch, and F. Huisken, "CARS spectroscopy of molecules and clusters in supersonic jets," Appl. Phys. B **45**(4), 205–214 (1988).
51. H.-D. Barth and F. Huisken, "Investigation of librational motions in gas-phase CO_2 clusters by coherent raman spectroscopy," Chem. Phys. Lett. **169**(3), 198–203 (1990).
52. H.-D. Barth, F. Huisken, and A. A. Ilyukhin, "Coherent raman spectroscopy of nitrogen molecules and clusters in supersonic jets," Appl. Phys. B **52**(2), 84–89 (1991).